Carbohydrate Polymers 84 (2011) 881–886

Contents lists available at ScienceDirect

Carbohydrate Polymers

journal homepage: www.elsevier.com/locate/carbpol

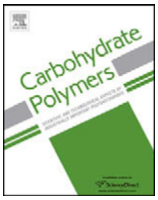

Concomitant degradation in periodate oxidation of carboxymethyl cellulose

Hongli Li[a], Bo Wu[b], Changdao Mu[a], Wei Lin[a,*]

[a] *Department of Pharmaceutics and Bioengineering, School of Chemical Engineering, National Engineering Laboratory for Clean Technology of Leather Manufacture, Sichuan University, Chengdu, Sichuan, China*
[b] *Hefei National Laboratory for Physical Sciences at Microscale, Department of Chemical Physics, University of Science and Technology of China, Hefei, Anhui, China*

ARTICLE INFO

Article history:
Received 24 September 2010
Received in revised form
23 November 2010
Accepted 8 December 2010
Available online 15 December 2010

Keywords:
Carboxymethyl cellulose
Periodate
Aldehyde content
Laser light scattering (LLS)
Wide angle X-ray diffraction (WAXD)
Atomic force microscopy (AFM)

ABSTRACT

Conversion of carboxymethyl cellulose (CMC) to its dialdehyde derivatives by periodate oxidization in acid solutions has been investigated as a function of pH, temperature, reaction time and periodate dosage. Our results show that the stoichiometric ratio of $NaIO_4$ to CMC and the pH of aqueous medium are substantially responsible for the aldehyde content and yield of the product. Laser light scattering (LLS) and wide angle X-ray diffraction (WAXD) measurements demonstrate that physical and chemical degradations concomitant with the oxidization process occur, leading to the decrease in $\langle R_h \rangle$ and crystallinity, respectively. The degradation mechanism for acid-catalyzed cleavage of β-1-4-glycosidic bond is proposed. Atomic force microscopy (AFM) images reveal the morphological changes of CMC with the degree of oxidization. The present study quantitatively indicates the substantial degradation in derivatization of cellulose by periodate oxidization method, and is helpful for exploring novel carboxymethyl polysaccharide derivatives.

1. Introduction

Carboxymethyl cellulose (CMC) is a commercial water-soluble cellulose ether, available in different degrees of substitution. As one of the major cellulose derivatives, CMC is non-toxic, biodegradable, cheap and widely used in many industrial sectors including food, textiles, paper, adhesives, paints, pharmaceutics, cosmetics and mineral processing (Ali, El-Rehim, Kamal, & Hegazy, 2008). In addition, CMC has recently been proved possess good biocompatibility, and is thus a promising biomaterial for biomedical application (Cook, Salkeld, & Patron, 2005; Jiang, Li, Zhang, & Wang, 2009). With respect to polysaccharide and protein composites, CMC is generally simply blended (Cheng, KarimA, & Seow, 2008; Lii, Tomasik, Zaleska, Liaw, & Lai, 2002) or cross-linked with gelatin by using glutaraldehyde as a crosslinker (Rokhade et al., 2006). In order to improve the functionality in existing applications, e.g. without employing any extraneous cross-linking agents, it is essential to increase the reactivity of CMC by molecular modification.

Periodate oxidation has long been industrially utilized in the production of dialdehyde starch and cellulose by specifically cleaving the C2–C3 bond of the 1,4-glucan unit (Jackson & Hudson, 1937; Potthast, Rosenau, & Kosma, 2006). With this method, a large number of aldehyde groups are introduced into polysaccharides and can be further converted to carboxylic acids, primary alcohols or imines (Schiff bases) with primary amines (Kim, Kuga, Wada, Okano, & Kondo, 2000). This makes the resulting compounds serve as useful intermediates for cellulose-based functional materials, such as an adsorbent of heavy metal, drug carriers, separation and analysis of protein (Kim & Kuga, 2001).

In this work, we prepared a series of dialdehyde CMC (DCMC) with varied aldehyde contents according to this reaction and thereby found significant degradation concomitant with the progressing periodate oxidization. However, the known data about the effect of the degradation on the yield of product and molecular conformation are still limited so far (Potthast, Rosenau, & Kosma, 2006). Therefore, the aim of this study is to analyze the crucial parameters that affect the degradation and explore the chemical degradation mechanism by use of laser light scattering (LLS), wide angle X-ray diffraction (WAXD) and atomic force microscopy (AFM).

2. Experimental

2.1. Materials

Carboxymethyl cellulose sodium (CMC) and sodium periodate were purchased from Kelong Chemical Reagent Company (Chengdu, China). The viscosity of the 2% (w/v) CMC in water was reported by the company to be ≥1200 mPa·s and confirmed in our laboratory. The degree of substitution (DS) was ~0.90 according to Fourier transform infrared (FTIR) analysis (Sannan, Kurita, Ogura, &

---

* Corresponding author. Tel.: +86 28 8546 0819; fax: +86 28 8540 5237.
E-mail address: wlin@scu.edu.cn (W. Lin).

0144-8617/$ – see front matter © 2010 Elsevier Ltd. All rights reserved.
doi:10.1016/j.carbpol.2010.12.026

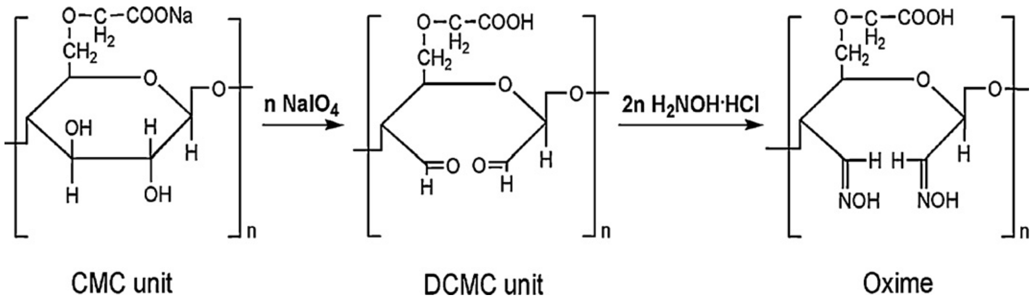

Fig. 1. The illustration of periodate oxidization of CMC to DCMC, and conversion of DCMC to oxime by Schiff base reaction with hydroxylamine hydrochloride.

Iwakura, 1978). The periodate was of analytical grade. All chemicals were used as received.

2.2. Preparation of dialdehyde carboxymethyl cellulose (DCMC)

About 1.0 g CMC was dissolved in 20 mL deionized water in the flask which was immersed in a DF-101S temperature controlled water bath with a magnetic stirrer (Shanxi Taikang Biotech., China). Then, 10 mL periodate solution at different concentrations was added to the CMC solution under stirring. The pH was adjusted with 1 M sulfuric acid solution. After the mixture was stirred in the dark at designated reaction temperature for a predetermined time, the oxidized product, referred to dialdehyde carboxymethyl cellulose (DCMC) was precipitated by pouring the solution into a large amount of ethanol. It was then recovered and cross-washed with distilled water and ethanol until all iodic compounds were removed. The reaction conditions were optimized against pH, temperature, reaction time and the mole ratio of periodate to CMC. The product was dried at 37 °C to constant weight for the subsequent measurements.

2.3. Determination of aldehyde content

The degree of oxidization of CMC was evaluated by the determination of the aldehyde content (Kim, Kuga, Wada, Okano, & Kondo, 2000; Veelaert, de Wit, Gotlied, & Verhe, 1997). The DCMC was converted to oxime by Schiff's base reaction with hydroxylamine hydrochloride, as shown in Fig. 1. In detail the procedures are as follows: ~0.5 g DCMC of known water content was dissolved in 25 ml distilled water and the pH was adjusted to 5 with sodium hydroxide (NaOH). Then 20 ml of 0.72 mol/L hydroxylamine hydrochloride ($H_2NOH{\cdot}HCl$) in pH 5 solution was added into the DCMC solution. The mixture was stirred for 4 h in the thermostated water bath at 40 °C, and then followed by titration of the released hydrochloric acid with 1.0 mol/L NaOH. Here, the consumption of NaOH solution in liter was recorded as V_c. The same concentration of CMC solution at pH 5 was used as a blank and its consumption of the alkali solution in liter was recorded as V_b. Thus, the aldehyde content (AC) in DCMC can be calculated by

$$AC\,(\%) = \frac{M_{\mathrm{NaOH}}\,(V_C - V_b)}{m/211} \times 100 \tag{1}$$

where $M_{\mathrm{NaOH}} = 1.0$ mol/L, m is dry weight of DCMC sample in g, and 211 is approximately the molecular weight of repeating unit in DCMC. Each set of the test was done in triplicate.

2.4. Fourier transform infrared spectral studies

Fourier transform infrared (FTIR) spectra of CMC and DCMC were obtained from discs containing ~2.0 mg dry sample in approximately ~200 mg potassium bromide (KBr). The measurements were recorded by a Perkin–Elmer Spectrum One FT-IR spectrophotometer at the resolution of 4 cm^{-1} in the wave number region 450–4000 cm^{-1}.

2.5. Laser light scattering measurements

The laser light scattering (LLS) measurements were conducted on a commercial LLS spectrometer (ALV/DLS/SLS-5022F) equipped with a multi-τ digital time correlator (ALV5000) and a cylindrical 22 Mw UNIPHASE He–Ne laser ($\lambda = 632$ nm) as the light source. In dynamic LLS (Beme & Pecora, 1976), the cumulative analysis of the measured intensity–intensity time correlation function $G^{(2)}(t,q)$ can result in a line-width diffusion coefficient distribution ($G(\Gamma)$) or an average line-width ($\langle\Gamma\rangle$). For diffusive relaxation, $\langle\Gamma\rangle$ is further related to the average translational diffusion coefficient ($\langle D\rangle$) of the scattering object in dilute solution by $\langle D\rangle = (\langle\Gamma\rangle/q^2)_{q\to 0}$, or the hydrodynamic radius ($\langle R_h\rangle$) by the Stokes–Einstein equation, $\langle R_h\rangle = k_B T/(6\pi\eta\langle D\rangle)$, with k_B, T, and η being the Boltzmann constant, the absolute solution temperature, and the solution viscosity, respectively. The hydrodynamic radius distribution $f(R_h)$ can also be calculated for the Laplace inversion of a corresponding measured $G^{(2)}(t,q)$ using the CONTIN program in the correlator. The details of the LLS instrument and theory can be found elsewhere (Chu, 1991; Xie, Bai, Xu, Bai, & Zhang, 2007). All dynamic LLS measurements were conducted at a scattering angle of 90°. The DCMC solutions were clarified using 0.45 μm hydrophilic Millipore millex filters. The concentration of the solutions was 5.0×10^{-3} g/mL. All LLS measurements were performed at 25 °C after the solution was equilibrated for 20 min.

2.6. X-ray diffraction measurements

Wide angle X-ray diffraction (WAXD) profiles were obtained using an 18 kW rotating anode X-ray diffractometer (MXPAHF, Japan) with a fixed Cu K_α radiation of 0.154 nm and a sample to detector distance of 10 cm. The sample was scanned in the range of diffraction angle (2θ) from 5° to 50° with a scanning rate of 2°/min at ambient temperature and humidity. The Peakfit4 (AISL software), one-dimensional peak fitting program, was used to determine the peak size shapes and the integrated intensity of the linear profiles.

Crystallinity index (CI), representing relative degree of crystallinity, was calculated from linear intensity profile according to the literature (Rowland & Cousins, 1966), using the relationship: $CI = (I_{002} - I_{\mathrm{am}})/I_{002} \times 100$, where I_{002} is the intensity in the diffraction profile at the position of the 002 peak ($2\theta = 22.7°$ for the samples) and I_{am} is the intensity at locations for the amorphous background ($2\theta = 38$–$40°$) (Segal, Creely, Martin, & Conrad, 1959).

2.7. Atomic force microscopy observations

Topographic images of CMC and DCMC on mica were observed by atomic force microscopy (AFM) on a Shimadzu SPM-9600 in dynamic mode at constant forces. After the samples were diluted to

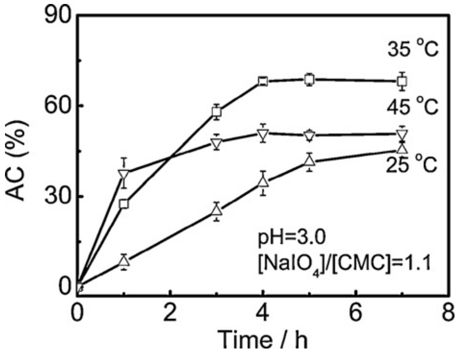

Fig. 2. The aldehyde content (AC) in DCMC as a function of reaction time at different oxidation temperature, where the pH was controlled at 3.0 and the mole ratio of $NaIO_4$ to CMC 1.1:1.

the concentration of 5×10^{-5} g/mL and equilibrated at 4 °C for 12 h, a droplet of the solution (5 μL) was dropped onto freshly cleaved mica. Then it was dried in the vacuum-desiccator for 24 h. All the AFM measurements were performed under ambient condition at room temperature.

3. Results and discussion

Periodate oxidation under acidic conditions or the Malaprade reaction, is known to be a highly specific reaction to convert 1,2-dihydroxyl groups (glycol) to paired aldehyde groups without significant side reactions (Potthast, Rosenau, & Kosma, 2006). During the oxidation, 1 mol of CMC theoretically consumes 1 mol of $NaIO_4$, as shown in Fig. 1 (Fang, Takahashi, & Nishinari, 2005). It was demonstrated that the oxidation degree of CMC can be quantitatively manipulated by controlling the preparation parameters. Note that the degree of oxidation, which corresponds with the aldehyde content (AC), is generally determined by the method of alkali consumption based on Cannizzaro reaction (Potthast, Rosenau, & Kosma, 2006), whereas this method is not appropriate to determine DCMC owing to the interference of the side carboxyl groups. The AC value is therefore approximated by measuring the amount of reactive aldehydes available for oxime formation, also schematically shown in Fig. 1. For dialdehyde starch (Veelaert, de Wit, Gotlied, & Verhe, 1997), a maximum value of about 80% of the total aldehydes was obtained in conversion into oximes. And the rest unavailable aldehyde groups are attributed to the formation of hemiacetal and acetal groups that protect the aldehyde from further reactions. In our present study, the similar results are observed for DCMC, namely, the maximum value of the measured AC is ~81% of the total aldehydes.

Fig. 2 shows the measured AC in DCMC as a function of reaction time under super-stoichiometric ratio of periodate, i.e., the mole ratio of $NaIO_4$ to CMC 1.1. At the oxidation temperature of 45 °C, the maximum oxidization extent is reached after ~3 h, whereas at 35 °C it needs ~4 h but the plateau value is higher than that of the former. And at 25 °C, the plateau of AC corresponds to ~7 h at a lowest level. Increasing temperature is favorable for the periodate oxidization at the beginning due to the nature of the endothermic reaction. However, high temperature will cause the decomposition of periodate and thus the effect of the oxidant is lost more or less. This can explain the lower AC plateau at 45 °C than at 35 °C.

The change of pH is expected to affect the system substantially. For preparation of dialdehyde starch by oxidization with periodate, the pH range was controlled between 3 and 7. (Veelaert, de Wit, Gotlied, & Verhe, 1997) Note that the oxidization reaction is catalyzed by the presence of H^+. On the other hand, the physical and chemical degradations in extremely acid media (Jackson & Hudson, 1938; Wilham, McGuire, & Mehltretter, 1971) result in the lower yield of the product. Therefore, an optimum pH value is expected for production of DCMC. Fig. 3 shows the effects of pH on the degree of oxidation and the yield of product at three mole ratios of $NaIO_4$ to CMC. Indeed at pH 2, there exists a highest AC value (81%) which is nearly independent of the excessive periodate amount. However, the yield at this point is even less than 50%. On the whole, the yield approaches to the plateau at pH 3.0 and higher values, although the AC values start to decline here with further increasing pH. Moreover, the plateaus of yields at super-stoichiometric ratio of $NaIO_4$ are lower instead. It suggests that the excessive oxidization would lead to the degradation of CMC or DCMC. The further interpretation will be discussed later. Therefore, the periodate oxidization of CMC is performed at $T = 35$ °C, pH 3.0 for 4 h with varied mole ratios of $NaIO_4$/CMC to introduce different content of aldehyde in the subsequent investigations.

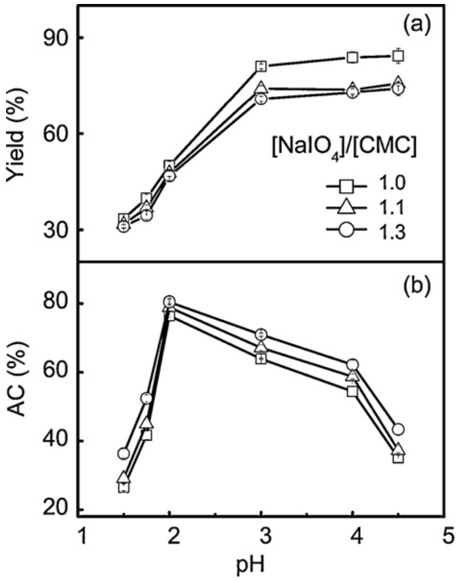

Fig. 3. The aldehyde content (AC) and the yield of DCMC as a function of pH at different oxidant dosage, where reaction temperature and time are 35 °C and 4 h, respectively.

Fig. 4 shows the FTIR spectra of CMC before and after the oxidization. It is clear that two characteristic IR bands at ~1738 cm^{-1} and ~886 cm^{-1} regions appear in oxidized CMC, namely DCMC. Moreover, both intensities markedly increase with increasing degree of oxidation, which is consistent with the reported FTIR spectra of periodate oxycellulose (Calvini, Gorassini, Luciano, & Franceschi, 2006; Fan, Lewis, & Tapley, 2001; Kim, Kuga, Wada, Okano, & Kondo,

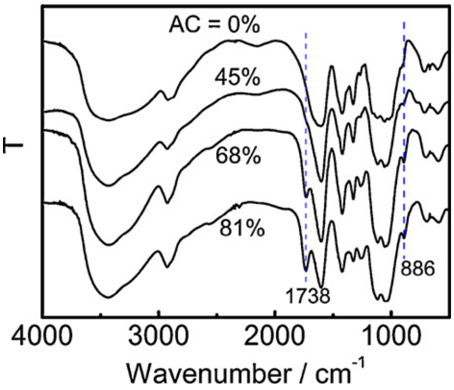

Fig. 4. FTIR spectra for CMC and DCMC with different aldehyde contents, i.e., AC = 0%, 45%, 68%, and 81%, respectively.

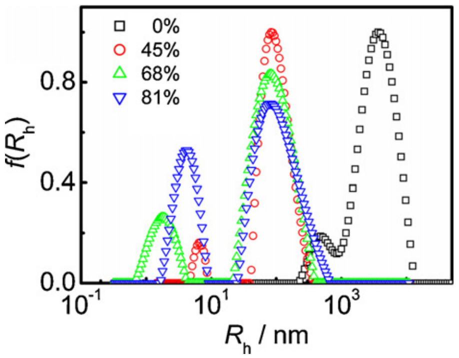

Fig. 5. Typical hydrodynamic radius distributions $f(R_h)$ of CMC and DCMC with different aldehyde contents, i.e., AC = 0%, 45%, 68%, and 81%, respectively, measured by dynamic LLS at 25.0 °C.

2000). Generally, the absorbance at about 1740 cm^{-1} is characteristic of aldehydic carbonyl groups, while the band around 880 cm^{-1} is assigned to the formation of hemiacetal bonds between the aldehyde groups and neighbor hydroxyl groups. The results indicate that the aldehyde group has been introduced into the structure by selective periodate oxidation of CMC.

Fig. 5 shows the hydrodynamic radius distributions $f(R_h)$ of CMC and DCMC with different aldehyde contents measured by dynamic LLS. It exhibits bimodal distribution for all the species. The distinct much higher $\langle R_h \rangle$ distribution for CMC indicates that the molecules form aggregates in aqueous solution due to the existence of hydrogen bonding. The intermolecular hydrogen bonds are believed to be the primary factor holding the cellulose chains together forming the fibrous structure (Xiang, Lee, Pettersson, & Torget, 2003). The state of hydrogen bonding also determines other physical properties of cellulose, such as the extent of crystallinity. When the CMC is oxidized, both of the peaks at ~450 and ~4000 nm shift greatly to lower positions. In addition, as the extent of oxidization increase, the main peaks at ~83 nm slight change, but the intensity of smaller peaks in the region <10 nm increase apparently, suggesting that the disruption of bulk DCMC leads to short fragments during periodate oxidization. The former could be attributed to the breaking of hydrogen bonds, and the latter is small degradation products. Obviously, the higher the aldehyde content or oxidization level, the more degradation occurs. This result can explain the determined lower yields at higher AC values under the same oxidization temperature and time (Fig. 3).

As discussed before, periodate oxidation of polysaccharides like starch and cellulose is generally characterized by its selective cleavage of the carbon–carbon bond between vicinal hydroxyl groups of the anhydro D-glucopyranose residues, giving a ring-opened product containing two aldehyde groups. Although there are many reports related to application of this reaction, seldom has discussed or quantitatively understood the degradation concomitant with the progressing oxidization. It is generally recognized that the dialdehyde form is more susceptible to hydrolytic attack than the unmodified cellulose (Maekawa & Koshijima, 1991), and acid treatment is considered to degrade the oxidized parts preferentially (Kim, Kuga, Wada, Okano, & Kondo, 2000). However, the degradation mechanism in acidic media for dialdehyde starch or cellulose has not established because of the difficulty to definite identification of all degradation mixtures (Veelaert, de Wit, Gotlied, & Verhe, 1997). In fact, during oxidative treatment of pulp materials with ozone, peroxide or hypochlorite in papermaking, cellulose degradation is involved as reflected by decreasing M_w (Potthast, Rosenau, & Kosma, 2006). In our experiments, we do observe a significant decrease in $\langle R_h \rangle$ of CMC and an increase in very small molecules portion of DCMC as increasing degree of oxidization by dynamic LLS, revealing the more or less inevitable degradation of CMC when converted into DCMC. It has been proved that the complete hydrolysis of dialdehyde polysaccharides under strong acid and high temperature (~100 °C) results in D-erythrose and glyoxal (Jackson & Hudson, 1938; Wilham, McGuire, & Mehltretter, 1971). While under relatively mild conditions in the present study, the chemical degradation mechanism can be acid-catalyzed cleavage of β-1-4-glycosidic bond, which follow the pattern outlined in Fig. 6. Note that it does not exclude the possible presence of other types of reactions due to the complexity of natural biomass. The degradation of DCMC could proceed in three steps, similar to the acid hydrolysis of cellulose (Xiang, Lee, Pettersson, & Torget, 2003).

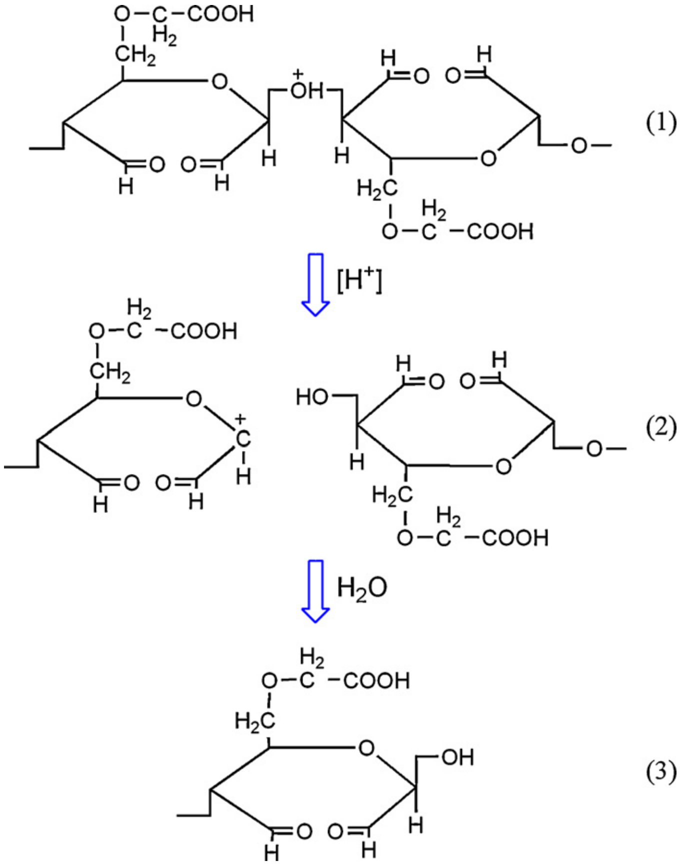

Fig. 6. Mechanism of acid-catalyzed hydrolysis of DCMC by cleavage of β-1-4-glycosidic bond: (1) protonation of the glycosidic oxygen linking two sugar units under acidic condition; (2) cleavage of the C-O bond and formation of the carbonium ion; (3) the resulted segments and a proton are liberated by addition of water.

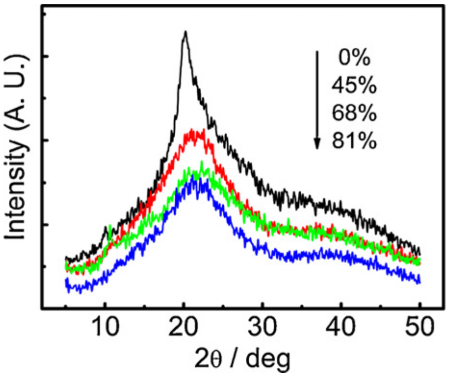

Fig. 7. Wide angle X-ray diffraction linear intensity profile of CMC and DCMC with different aldehyde contents, i.e., AC = 0%, 45%, 68%, and 81%, respectively.

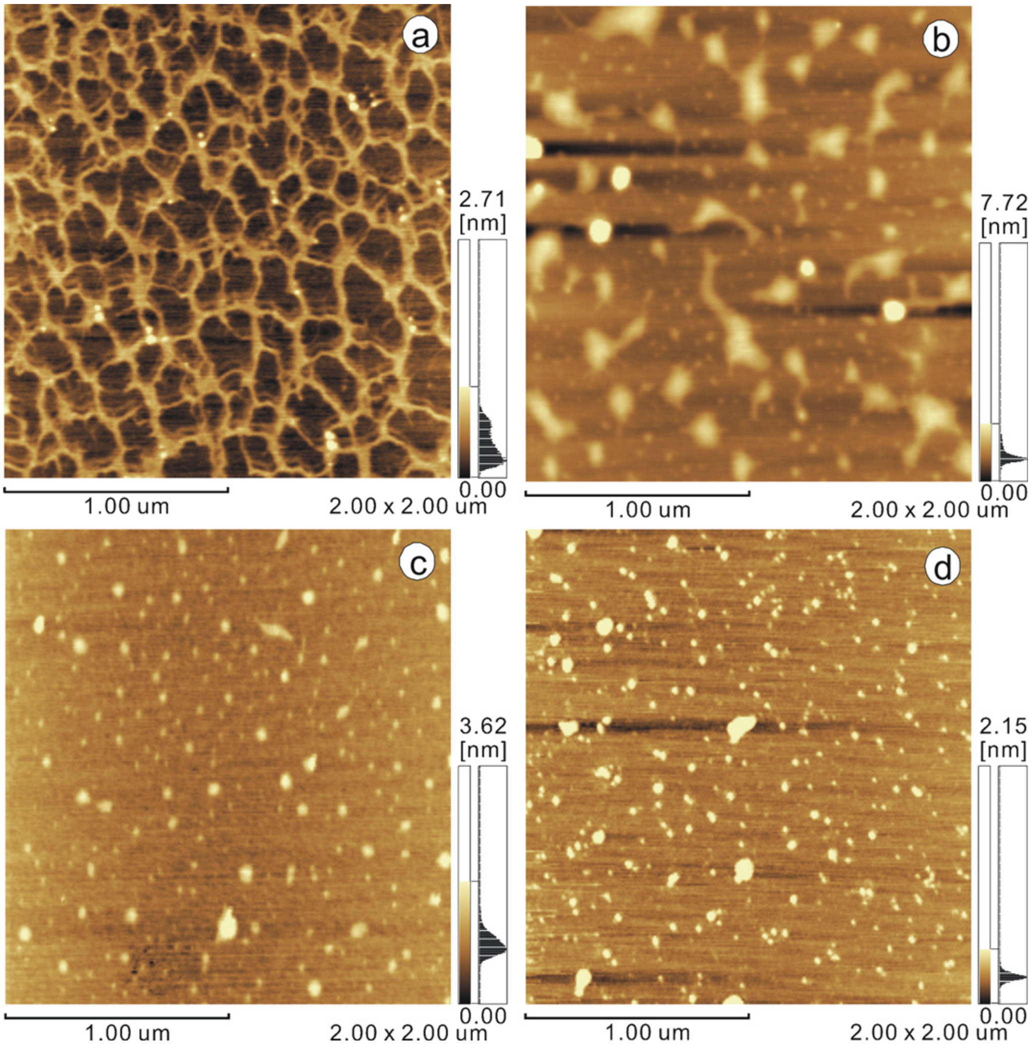

Fig. 8. AFM images of CMC (a) and DCMC with different aldehyde contents (AC): (b) 45%; (c) 68%; (d) 81%.

Firstly, the glycosidic oxygen linking two sugar units is rapidly protonated under acidic condition, forming a conjugate acid. Then the cleavage of the C–O bond and breakdown of the conjugate acid to the carbonium ion take place. After a rapid addition of water, the resulted segments and a proton are liberated. Assuming that the cleavage of the C–O bond takes place more rapidly at the end than in the middle of the polysaccharide chain, more monosaccharides and lower yields of DCMC are resulted, meanwhile the $\langle R_h \rangle$ of the macromolecules change slightly as reflected in Fig. 5.

To understand the effect of periodate oxidation on the degree of crystallinity, we examined the CMC and DCMC with different aldehyde contents by WAXD. Fig. 7 shows the WAXD linear intensity profiles of the samples versus diffraction angle. The peak at $2\theta = 22.7^\circ$ for CMC reveals the characteristic semi-crystalline nature (Zhao et al., 2009). Based on it, the measured crystallinity index (CI = 80%, 70%, 64% and 61%, respectively) decrease almost proportionately to the oxidation level of the starting CMC (AC = 0%, 45%, 68%, and 81%, respectively), accompanied by slight line broadening. The loss of crystallinity is considered to result from opening of glucopyranose rings and destruction of their ordered packing (Kim, Kuga, Wada, Okano, & Kondo, 2000). Therefore, the higher the oxidation level, the lower the degree of crystallinity. Meanwhile, the line broadening of the peak suggests that the periodate oxidation reaction occurs with almost equal facility in both the amorphous and crystalline regions of the cellulose (Varma, Jamdade, & Nadkarni, 1985). Kim, Kuga, Wada, Okano, and Kondo (2000) investigated the influence of this oxidation in the crystalline domains. Besides the decrease in crystallinity, it was proposed that the oxidation proceeds highly heterogeneously, forming isolated oxidized domains which are more sensitive to acid or alkali. Our results agree with the above conclusion.

Fig. 8 shows the AFM morphological changes of CMC induced by oxidization. Before oxidization, the entangled fibrous network topography is observed similar to the reported topographical image (Ueno, Yokota, Kitaoka, & Wariishi, 2007), indicating the aggregation of the CMC molecules. After periodate oxidization, the ordered aggregations on mica cannot be observed, the conformational heterogeneity of DCMC appears instead. Furthermore, as the oxidization level increases, the short fragments increase because of the degradation. The AFM images further prove previous LLS measurements.

4. Conclusion

The studies on the chemical and physical transitions of periodate oxidized CMC in aqueous media can lead to the following conclusions. The optimal oxidization conditions is found at the temperature of 35 °C, pH = 3.0 for 4 h, with a $NaIO_4$/CMC molar ratio of 1: 1. Super-stoichiometric $NaIO_4$ and lower pH (<3.0) result in higher aldehyde content but lower yield of the product (DCMC) due to degradations. As the degree of oxidization increases, physical degradation occurs owing to the breaking of intermolecular hydrogen bonds; and chemical degradation could be attributed to the cleavage of β-1-4-glycosidic bond catalyzed by acid. The concomitant oxidization and degradation lead to the decrease in crystallinity of DCMC and the conformational heterogeneity. The results make significance in understanding the degradation reaction accompanied with periodate oxidization during the development of functional cellulose derivatives.

Acknowledgements

The financial support of National Natural Science Foundation (NNSF) of China (20704028 and 21074074), and Science and Technology Planning Project of Sichuan Province (2010HH0004) is gratefully acknowledged. We thank Innovation Center for Postgraduates at HFNL, USTC, for supporting the LLS and WAXD measurements.

References

Ali, A. E. H., El-Rehim, H. A. A., Kamal, H., & Hegazy, D. E. S. A. (2008). Synthesis of carboxymethyl cellulose based drug carrier hydrogel using ionizing radiation for possible use as site specific delivery system. *Journal of Macromolecular Science. Part A: Pure and Applied Chemistry*, *45*, 628–634.

Beme, B., & Pecora, R. (1976). *Dynamic light scattering*. New York: Plenum Press.

Calvini, P., Gorassini, A., Luciano, G., & Franceschi, E. (2006). FTIR and WAXS analysis of periodate oxycellulose: Evidence for a cluster mechanism of oxidation. *Vibrational Spectroscopy*, *40*, 177–183.

Cheng, L. H., Karim, A. A., & Seow, C. C. (2008). Characterisation of composite films made of konjac glucomannan (KGM), carboxymethyl cellulose (CMC) and lipid. *Food Chemistry*, *107*, 411–418.

Chu, B. (1991). *Laser scattering*. New York: Academic Press.

Cook, S. D., Salkeld, S. L., & Patron, L. P. (2005). Bone defect healing with an osteogenic protein-1 device combined with carboxymethylcellulose. *Journal of Biomedical Materials Research. Part B: Applied Biomaterials*, *75*, 137–145.

Fan, Q. G., Lewis, D. M., & Tapley, K. N. (2001). Characterization of cellulose aldehyde using Fourier transform infrared spectroscopy. *Journal of Applied Polymer Science*, *82*, 1195–1202.

Fang, Y. P., Takahashi, R., & Nishinari, K. (2005). Protein/polysaccharide cogel formation cased on gelatin and chemically modified schizophyllan. *Biomacromolecules*, *6*, 3202–3208.

Jackson, E. L., & Hudson, C. S. (1937). Application of the cleavage type of oxidation by periodic acid to starch and cellulose. *Journal of the American Chemical Society*, *59*(10), 2049–2050.

Jackson, E. L., & Hudson, C. S. (1938). The structure of the products of the periodic acid oxidation of starch and cellulose. *Journal of the American Chemical Society*, *60*(5), 989–991.

Jiang, L. Y., Li, Y. B., Zhang, L., & Wang, X. J. (2009). Preparation and characterization of a novel composite containing carboxymethyl cellulose used for bone repair. *Materials Science and Engineering C*, *29*, 193–198.

Kim, U. J., & Kuga, S. (2001). Ion-exchange chromatography by dicarboxyl cellulose gel. *Journal of Chromatography*, *919*, 29–37.

Kim, U. J., Kuga, S., Wada, M., Okano, T., & Kondo, T. (2000). Periodate oxidation of crystalline cellulose. *Biomacromolecules*, *1*, 488–492.

Lii, C. Y., Tomasik, P., Zaleska, H., Liaw, S. C., & Lai, V. M. F. (2002). Carboxymethyl cellulose–gelatin complexes. *Carbohydrate Polymers*, *50*, 19–26.

Maekawa, E., & Koshijima, T. (1991). Preparation and structural consideration of nitrogen-containing derivatives obtained from dialdehyde celluloses. *Journal of Applied Polymer Science*, *42*, 169–178.

Potthast, A., Rosenau, T., & Kosma, P. (2006). Analysis of oxidized functionalities in cellulose. *Advance in Polymer Science*, *205*, 1–48.

Rokhade, A. P., Agnihotri, S. A., Patil, S. A., Mallikarjuna, N. N., Kulkarni, P. V., & Aminabhavi, T. M. (2006). Semi-interpenetrating polymer network microspheres of gelatin and sodium carboxymethyl cellulose for controlled release of ketorolac tromethamine. *Carbohydrate Polymers*, *65*, 243–252.

Rowland, S. P., & Cousins, E. R. (1966). Periodate oxidative decrystallization of cotton cellulose. *Journal of Polymer Science: Part A-1*, *4*, 793–799.

Sannan, T., Kurita, K., Ogura, K., & Iwakura, Y. (1978). Studies on chitin: 7. I.R. spectroscopic determination of degree of deacetylation. *Polymer*, *19*, 458–459.

Segal, L., Creely, J. J., Martin, A. E., & Conrad, C. M. (1959). An empirical method for estimating the degree of crystallinity of native cellulose using the X-ray diffractometer. *Textile Research Journal*, *29*, 786–794.

Ueno, T., Yokota, S., Kitaoka, T., & Wariishi, H. (2007). Conformational changes in single carboxymethylcellulose chains on a highly oriented pyrolytic graphite surface under different salt conditions. *Carbohydrate Research*, *342*, 954–960.

Varma, A. J., Jamdade, Y. K., & Nadkarni, V. M. (1985). Wide-angle X-ray diffraction study of the effect of periodate oxidation and thermal treatment on the structure of cellulose powder. *Polymer Degradation and Stability*, *13*, 91–98.

Veelaert, S., de Wit, D., Gotlied, K. F., & Verhe, R. (1997). Chemical and physical transitions of periodate oxidized potato starch in water. *Carbohydrate Polymers*, *33*, 153–162.

Wilham, C. A., McGuire, T. A., & Mehltretter, C. L. (1971). Hydrolysis of dialdehyde starch with sulfurous acid. *Starch*, *23*, 201–203.

Xiang, Q., Lee, Y. Y., Pettersson, P. O., & Torget, R. (2003). Heterogeneous aspects of acid hydrolysis of α-cellulose. *Applied Biochemistry and Biotechnology*, *105–108*, 505–514.

Xie, D. H., Bai, W., Xu, K., Bai, R. K., & Zhang, G. Z. (2007). Polymeric micelles formed by splitting of micellar cluster. *The Journal of Physical Chemistry B*, *111*(28), 8034–8037.

Zhao, Q., Qian, J. W., An, Q. F., Gui, Z. L., Jin, H. T., & Yin, M. J. (2009). Pervaporation dehydration of isopropanol using homogeneous polyelectrolyte complex membranes of poly(diallyldimethylammonium chloride)/sodium carboxymethyl cellulose. *Journal of Membrane Science*, *329*, 175–182.